Influence of Molecular Weight on the Domain Coarsening Rates in Linear Polyethylene–Poly(ethylene-*co*-1-octene) Blends

Noree Phochalam, Arunee Tabtiang, Richard A. Venables

Faculty of Science, Mahidol University, Rama VI Road, Bangkok 10400, Thailand

Received 29 October 2002; accepted 27 January 2003

ABSTRACT: The coarsening rates of the two-phase morphologies of linear polyethylene/poly(ethylene-*co*-1-octene) blends were determined as functions of molecular weight. Samples with cocontinuous morphologies that were prepared through solution blending were annealed in the melt state for various times, and ,subsequently the length scales of the morphologies were determined with a line-intersection method. Length-scale data were multiplied by a function that normalized for the effects of differences in zero-shear-rate viscosity and thermal energy; after normalization, the data largely fell on one trend line within the bounds of experimental error. This indicated that the principal effect of increasing molecular weight was to slow the coarsening rate through an increase in melt viscosity, with little effect from the thermodynamic compatibility of the two polymers. J Appl Polym Sci 90: 1655–1661, 2003

Key words: polyolefins; blends; morphology; metallocene catalysts; polyethylene (PE)

INTRODUCTION

Mixing, phase separation, and domain coarsening affect the morphology[1] and, hence, the properties of polyolefin blends.[2] The principal factors that affect these characteristics in polyolefin blends are molecular weight and the type and level of branching, the latter being largely controlled by the type and quantity of comonomer present. The thermodynamics of these systems have been described[3] by an empirical interaction parameter (χ) as a function of branch content, where χ is found by the fitting of the experimental data to various models. This has been accomplished through small-angle neutron-scattering studies with random-phase approximation[4] or by cloud-point determination.[5] In the latter approach, because the refractive indices of polyolefins are closely matched, the cloud point could be inferred from the morphology of annealed and quenched samples. The invariance with time of domain size of a fine length-scale morphology is indicative of a single-phase melt, whereas increases in domain size on annealing reveal a two-phase melt.[6] Results have been presented, however, where laser light scattering was used to study the length scale (λ) of mixing and coarsening in blends of isotactic polypropylene and poly(ethylene-*co*-propylene)[7] and for blends of isotactic polypropylene or syndiotactic polypropylene with poly(ethylene-*co*-propylene-*co*-ethylene norborene).[8]

One of the explanations of χ was based on regular solution theory, whereby differences in the solubility parameter of the constituent polymers led to an enthalpy-based factor. Several studies on polyolefin blends have shown that the number of branches in the molecule has the most important effect on the determination of the miscibility and compatibility of nonpolar polyolefin blends. It has been proposed that mixing in polyolefin blends may be related to enthalpic considerations that can be described by solubility parameters. Choi[9] calculated the Hildebrand solubility parameters (δ's) at elevated temperatures of 1000 simulated carbon models of linear polyethylene (PE) and poly(ethylene-*co*-1-butene) copolymers, the latter possessing between 10 and 80 ethyl branches per 1000 carbon backbone atoms. An abrupt increase in χ was found in the range 40–50 ethyl branches per 1000 carbon backbone atoms, where χ was calculated from $\chi = V_0R^{-1}T^{-1}(\delta_1 - \delta_2)^2$, where χ is the interaction parameter, V_0 is the reference volume, R is the gas constant, and T is absolute temperature. This was associated with the onset of macroscopic phase separation in the melt state. Krishnamoorti et al.[10] related solubility parameter analysis and solubility parameters determined from pressure–volume–temperature relationships for a series of blends comprising hydrogenated polydienes, which were used as model polyolefins with different branch types and contents, to their mixing behaviors as determined through small-angle neutron scattering. It was concluded that because solubility parameters could uniquely be as-

Correspondence to: R. A. Venables (frrav@mahidol.ac.th).
Contract grant sponsor: Thailand Research Fund.

TABLE I
Resin Characteristics and Their Corresponding Carreau Equation Constants at 170°C

Resin	Sample	MFI[a] (dg min^{-1})	α[b] (mol %)	M_w (kg mol^{-1})	M_n (kg mol^{-1})	η_0^* (Pas)	τ[c] (s)	n[d]
PE	PE1	42	0	101	39	383	0.021	0.469
PE	PE2	14	0	154	42	1,693	2.449	0.186
PE	PE3	0.9	0	234	—	14,061	1.143	0.312
EcO	EcO1	5.0	7.3	172	78	17,401	—	0.167
EcO	EcO2	0.5	7.3	261	123	42,183	0.001	0.263

M_w = weight-average molecular weight; M_n = number-average molecular weight.
[a] MFI = Melt flow index determined in accordance with BS 720A Test condition 4.
[b] α-olefin content.
[c] Reciprocal transition rate of the Carreau equation, eq. (1).
[d] Slope of the viscosity curve in the pseudoplastic region at $\dot{\gamma} \to \infty$. eq. (1).

signed to individual polyolefins, there were no specific pair interactions in most of the blends studied. The two methods of solubility parameter assessment gave numerical agreement with one another. Reductions in the entropy of mixing because of nonrandom effects that were related to differences in chain conformation and chain stiffness were considered by Bates et al.[5] The latter effect was described in terms of differences in the statistical segments of the blend constituents that were affected by branch length and comonomer content. Krishnamoorti et al.[10] reported that statistical segment length difference gave an indication of mixing in the melt state, but a clear correlation with the essential parameter in the theory was not established. Evidently, for polyolefin blends close to the limits of miscibility, there is a fine balance of these factors. Continuing from these studies, this study was centered on the influence of chain branching, because of the presence of a comonomer, and molecular weight on the compatibility and morphology of partially miscible polyolefin blends.

The objective of these experiments was to establish the influence of polymer molecular weight on the coarsening rates of the morphologies of selected polyolefin blends. Three commercial grades of high-density polyethylene (PE) and two poly(ethylene-*co*-1-octene) (EcO) resins that covered a wide range of molecular weights were chosen. PE was chosen because of the simplicity of its structure and its commercial importance.

EXPERIMENTAL

Materials

The PE samples were prepared with Zeigler–Natta catalysts,[11] and the EcO samples were synthesized with metallocene single-site catalysts.[12] Details of these resins are documented in Table I.

Characterization

Comonomer contents in the copolymers were determined with a Bruker 300-MHz NMR spectrometer (Karlsruhe, Germany) following the method of De Pooter et al.[13] Molecular weight data were obtained with a Waters gel permeation chromatograph (Milford, MA), with polystyrene calibration standards in trichlorobenzene at 142°C and a refractive index detector. Differential scanning calorimetry was carried out at heating rates of 5, 10, 15, and 20°C min^{-1} to determine the glass-transition temperatures (T_g's) of the copolymers with a PerkinElmer DSC-7 (Wellesley, MA). T_g at a heating rate of 0°C min^{-1} was estimated from the temperature axis intercept of the extrapolation to zero heating rate of the plot of T_g versus heating rate. Rheological data were obtained with a Haake RT20 rheometer with oscillating 25-mm parallel plates (Karlsruhe, Germany). Nineteen increments in the angular velocity (ω) were made over the range 0.06–64.3 rad s^{-1}. Measurements were made at 170°C under a constant stress of 250 Pa. Zero-shear-rate complex viscosity (η_0^*) was obtained from Carreau's constitutive equation:[14]

$$\eta_\omega^* = \frac{\eta_0^*}{(1 + \tau\omega)^n} \tag{1}$$

where η_ω^* is the complex viscosity at ω, τ is the relaxation time, and n is the non-Newtonian exponent; η_0^*, τ, and n were found from the unweighted least-sum-of-squares method[15] for the fit of the η_ω^* values experimentally determined through rheometry on the model containing ω as the independent variable; that is

$$ss_{\min} = \sum_{j=1}^{n} \Delta y_j^2 \tag{2}$$

where $ss_{\min}$ is the minimum sum of squares of n residuals, Δy_j is equal to $\eta_\omega^{*\prime} - \eta_\omega^*$, η_ω^* is the experimental value, and $\eta_\omega^{*\prime}$ is the corresponding value calculated from the model for datum j. The Solver program in Microsoft Excel '97 spreadsheet software was used to accomplish this task. For the EcO resin, a better fit of the experimental data was obtained with a modified Carreau equation by Dumoulin et al.:[16]

TABLE II
Blend Characteristics at 170°C

Blend	ϕ^a	ϕ_c	η_0^* (Pas)	τ^b (s)	n^c	$\eta_r{}^d$
PE1/EcO1	0.43	0.43	910	0.125	0.256	0.022
PE2/EcO1	0.49	0.49	1,656	0.207	0.264	0.097
PE1/EcO2	0.38	0.38	2,570	0.260	0.367	0.009
PE2/EcO2	0.44	0.43	5,530	0.360	0.443	0.040
PE3/EcO2	0.45	0.48	17,026	1.972	0.268	0.333

[a] Experimental volume fraction of EcO.
[b] Reciprocal transition rate of the Carreau equation, eq. 1.
[c] Slope of the viscosity curve in the pseudoplastic region at $\dot{\gamma} \rightarrow \infty$: eq. (1).
[d] Viscosity ratio, where $\eta_r = \eta^*_{0(PE)}/\eta^*_{0(EcO)}$.

$$\eta^*_\omega = \eta^*_0[1 + (\tau\omega)^n]^{-m} \quad (3)$$

where m is a fitting constant. The blends, listed in Table II, of PE with the copolymers were prepared with nominal compositions around the critical volume fraction of copolymer, as explained in the Discussion section, nominally around a volume fraction of 0.4.

The blends were prepared through dissolution of the components in toluene at 127°C followed by precipitation through pouring into excess methanol at 30°C. The precipitates were removed from the solvent through filtration and then washed with fresh methanol and left in the draft of a fume cupboard for 1 day before they were dried *in vacuo* at 80°C for 3 h. The samples were then consolidated and annealed in a in-house constructed tube furnace under a nitrogen gas purge for set times at 170°C. A thermocouple was inserted into the sample to determine the temperature. In some instances, samples were wrapped in aluminum and suspended in a temperature-controlled Haake recirculating oil bath at 170 ± 0.1°C for various times. The samples were then quenched in ice water and were sectioned to a nominal thickness of 1 μm with an RMC ultramicrotome (Manchester, England) operated at −80°C. The sections were placed upon glass slides beneath cover slips with dioctylphthalate as the mounting medium and were viewed with a Nikon E400 light microscope (Melville, NY) with phase-contrast plates. Images were captured with a Sony CMA-D2CE charged coupled device camera (CCD) and capture board (San Diego, CA). An additional group of blend samples was annealed for 6 h at temperatures in the range 150–350°C in a tube furnace under nitrogen flow. After they were quenched in ice water, flat surfaces were prepared with an RMC ultramicrotome and glass knife at −80°C. These surfaces were etched with a permanganic acid reagent (1.0% w/v solution at 30°C), following the method of Olley and Basset,[17] to selectively remove the amorphous material and were viewed with a Hitachi S-2360N scanning electron microscope (Los Angeles, CA) after vapor deposition with a platinum–palladium alloy.

λ of the observed morphologies was determined with Imagepro software (Silver Spring, MD). This method is illustrated in Figure 1, with the placement of chords over an image of a PE/EcO blend and the measurement of an intercept length (l), where $\lambda = \Sigma n_i l_i / n$, shown. Selected microscope images were converted to a frequency-based image by application of the Fourier transform. The frequency-based image comprised a cloud of points, the brightness of which represented the amplitude of the waveform and the position of which represented the frequency of the waveform. If the original image contained a regular pattern, the transformed image would show a regular pattern. For irregular images, a mass of dots would be seen that becomes brighter the closer they were to the center.

RESULTS AND DISCUSSION

Compatibility of the PE/EcO blend

Blend samples were annealed for various times at temperatures in the range 150–350°C in a tube furnace to determine the mutual melt-state compatibility of the PE and EcO. These samples were then quenched, microtomed, etched, and viewed with a scanning electron microscope; the resultant micrographs are shown in Figure 2. A plot of the number-average EcO-rich domain diameter (D_n) versus annealing temperature (T_a), as determined from the micrographs of Figure 2, is displayed in Figure 3. For all of the samples at every temperature, λ of the morphology coarsened on annealing, suggesting that all of the samples were in a two-phase state in the melt[18] because the morphologies coarsened to reduce the interfacial area between the phases and, hence, to minimize the interfacial

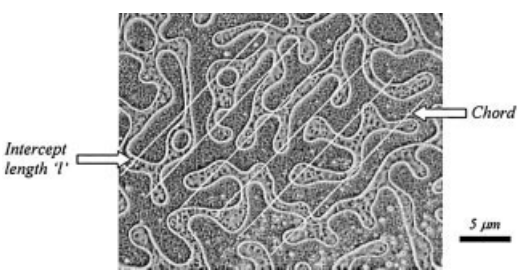

Figure 1 Line interception method to find λ of the cocontinuous morphologies.

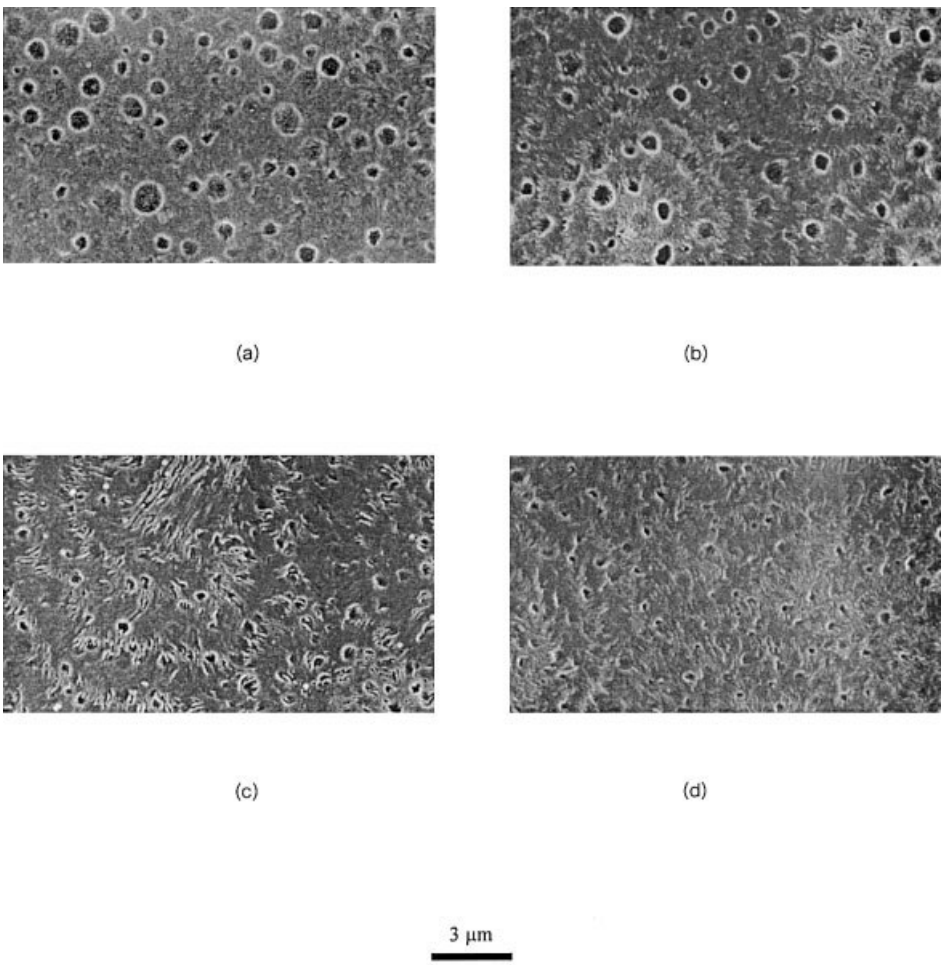

Figure 2 Scanning electron micrographs of the PE2/EcO2 blends containing 20 wt % EcO2 after annealing for 6 h at (a) 150, (b) 230, (c) 285, and (d) 320°C.

energy, that is, the product of the interfacial tension ($\Gamma_{1,2}$) and the interfacial area. Moreover, the extent of coarsening decreased as T_a increased, even though the mobility of the system increased with increasing temperature because of reduced viscosity, indicating enhanced compatibility at higher temperatures. In an earlier study,[19,20] we concluded that the PE2/EcO2 blend was partially miscible because of the observation of PE lamellar crystals in the EcO-rich domains of the morphology. As described by Rhee and Crist,[6] λ of the blend morphology is a function of the ratio χ/χ_c, where χ is the polymer–polymer interaction parameter and the subscript c refers to the critical point; that is, the thermodynamic force that drives the morphology to coarsen is weakened as the depth of quench decreases. Thus, for the blends studied herein, a virtual critical point may have been located at a high temperature that was practically inaccessible due the limited thermal stabilities of the constituent polymers. Experiments were limited to 350°C because of the embrittlement of the specimens at temperatures above 350°C. For the T_a range experienced by the samples described herein, that is, in the range 150–320°C, the specimens appeared largely unchanged from their original state, exhibiting slight discoloration and no apparent embrittlement.

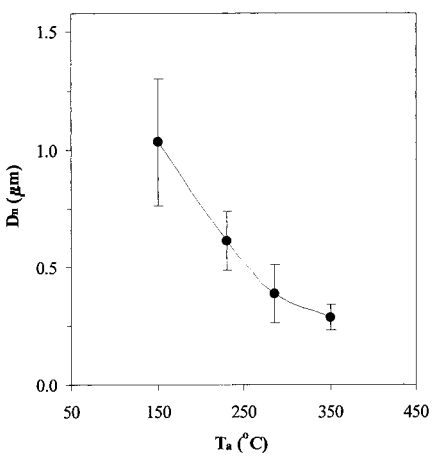

Figure 3 Plot of D_n versus T_a for the PE2/EcO2 blends containing 20 wt % EcO2 after annealing for 6 h at 170°C.

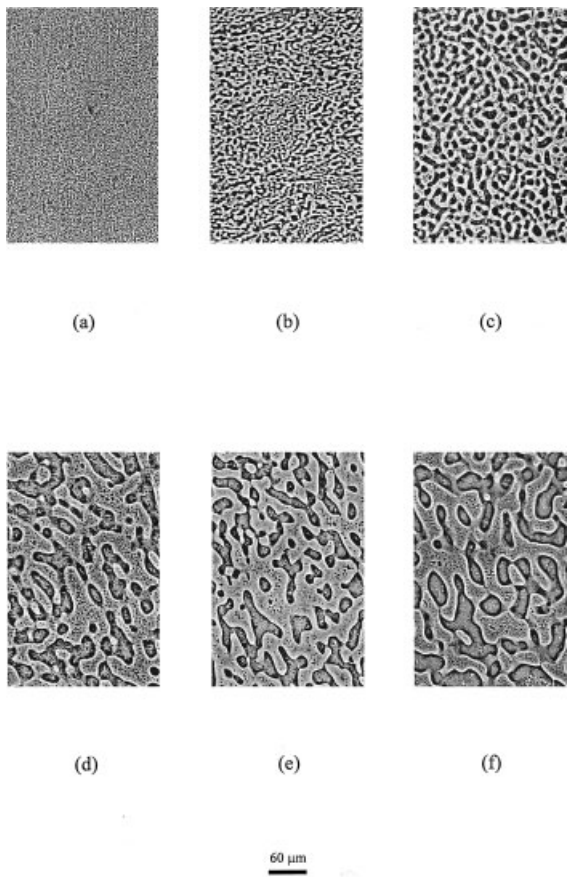

Figure 4 CCD images taken from the transmitted light microscope with a phase-contrast plate. Specimens comprised PE1/EcO1 at $\phi_c = 0.43$ for t's of (a) 5, (b) 15, (c) 30, (d) 60, (e) 90, and (f) 120 min at 170°C.

Coarsening rates

Because χ has been found to be a function of blend composition, particularly at low and high concentrations of polymer 2, where a twofold increase may occur,[6] the samples prepared for the coarsening rate study were prepared near the critical composition[21] to limit this effect; χ is generally near constant at compositions close to the critical point [the critical volume fraction of the EcO copolymer (ϕ_c)] from the Flory–Huggins lattice model:

$$\phi_c = [1 + (V_2 n_{w2}/V_1 n_{w1})^{1/2}]^{-1} \quad (4)$$

where V_j is the monomer volume and n_{wj} is the weight-average degree of polymerization of component j. On the basis of free-volume theory, V is a function of the expansion coefficient[22] (β) and T_g:

$$V_T = V_{298K}[1 + \beta_{298K}(T - 298)] \quad (5)$$

where β_{298K} is the thermal expansion coefficient at 298 K from[23]

$$\beta_{298K} = (298 + 4.23T_g)^{-1} \quad (6)$$

T_g values used were 253 and 203 K for EcO and PE, respectively. On annealing under quiescent conditions in the melt state at 170°C in an oil bath, the morphologies that formed were cocontinuous. Figure 4 shows examples of CCD images of selected PE1/EcO1 blends after annealing for various times. Figure 5 is an enlargement of a Figure 4(e) that reveals the nature of the phase domains. The phase contrast gave an impression of relief to the image; the apparently recessed regions contained circular ridges because of the presence of PE banded spherulites, identifying these regions as being PE-rich.

λ's of the morphologies are plotted as functions of annealing time (t) in Figure 6 for all of the samples prepared with compositions near the critical point. The characteristic λ of the morphology[6] is related to vector $\mathbf{q}$ by $\lambda = 2\pi/\mathbf{q}$. Plots of $\mathbf{q}$, on a natural logarithmic scale, versus the cubed root of annealing time ($t^{1/3}$) were essentially linear in the range $300 < t < 7200$ s, as shown in Figure 7.

Relationships of this type were discussed by Lee and Han,[24] who considered hydrodynamic effects during the early stage and late stages of coarsening, where

$$\lambda \propto (k_B T/\eta_0^*)^{1/3} t^{1/3} \quad (7)$$

and

$$\lambda \propto (\Gamma_{1,2}/\eta_0^*) t \quad (8)$$

respectively, where k_B is the Boltzmann constant and T is the absolute temperature. According to theories of spinodal decomposition[25] at times close to $t = 0$, $\mathbf{q}$ has a constant value of $\mathbf{q}_m$. The data presented here fall in the intermediate stage of coarsening, where λ is function of the cubed root of time. A normalized term ($\mathbf{q}^*$) may be defined as

$$\mathbf{q}^* = \mathbf{q}(k_B T/\eta_0^*)^{1/3} \quad (9)$$

which accounts for differences in thermal energy ($k_B T$) and viscous factors in the form of η_0^*. Examples of the

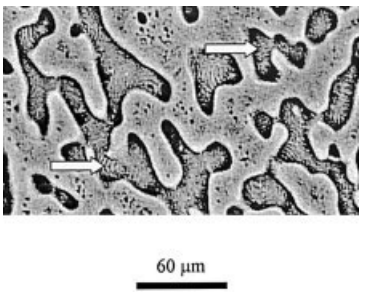

Figure 5 CCD image showing the presence of banded spherulites, indicated by arrows, and identifying the PE-rich domains, taken from a transmitted light microscope with a phase-contrast plate. The specimen comprised PE1/EcO1 at $\phi_c = 0.43$ annealed for 90 min at 170°C.

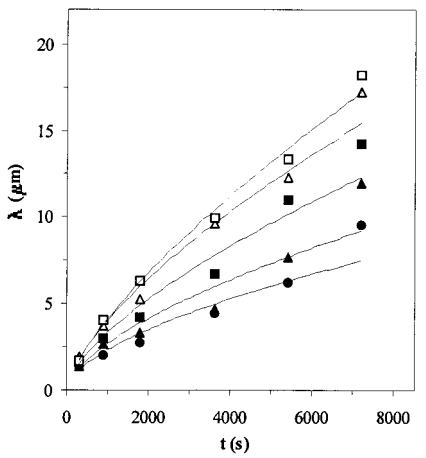

Figure 6 Plot of morphology λ versus t at 170°C for all of the blends prepared at the critical compositions: (■) PE1/EcO2, (▲) PE2/EcO2, (●) PE3/EcO2, (□) PE1/EcO1, and (△) PE2/EcO1.

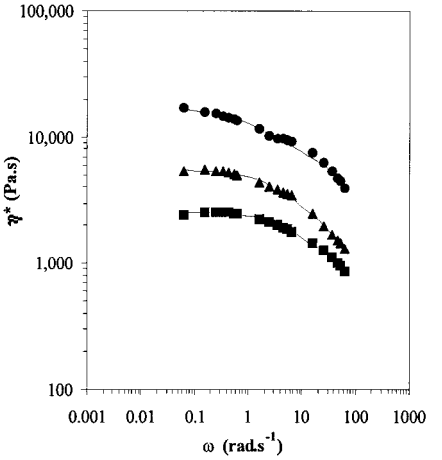

Figure 8 η^* versus ω flow curves at 170°C; trend lines were calculated with the least-sum-of-squares fit of the Carreau equation to the experimental data: (■) PE1/EcO2, (▲) PE2/EcO2, and (●) PE3/EcO2.

complex viscosity (η^*) versus frequency curves for these blends are shown in Figure 8. The **q*** function is plotted against $t^{1/3}$ in Figure 9. Apparently, normalization of the data with this function shifted the experimental data to lie close to a single curve, indicating that thermal energy and viscosity effects largely accounted for the differences in coarsening rates. In separate studies, Inaba et al.[7] and Lee and Han[24] reported that the coarsening in the melt state of immiscible blends after homogenization through dissolution of the constituent polymers in a common solvent and rapid precipitation with a nonsolvent was equivalent to phase separation via spinodal decomposition induced by deep quenching of a melt blend from a single-phase condition into a two-phase conditions through control of temperature and, hence, could be described through established kinetic models. The coarsening rate of the morphology (R) is

$$R = \mathbf{q}^2 D_{app}/2 \tag{10}$$

where the mutual diffusion coefficient (D_{app}) is defined by $D_{\text{app}} = D_s f$, in which D_s is the self-diffusion coefficient of polymer j, $D_j = k_j M_{(j)}^{-2}$, M is molecular weight, and

$$f = (\chi - \chi_s)/\chi_s \tag{11}$$

and is a factor that modifies the diffusion rates because of thermodynamic effects.[26] In this study, the blend compositions were close to the critical points, and hence, f may have been constant for each system. Zero-shear-rate viscosity and self-diffusion rates are closely related properties, with the term $(D/T)\eta_0$ being insensitive to temperature. Thus, $D_s \partial \eta_0^{-1}$, and, hence, $R \partial D_{\text{app}} \partial \eta_0^{-1} f$. Thus, the coarsening rate is largely controlled by the diffusion rate, which is a

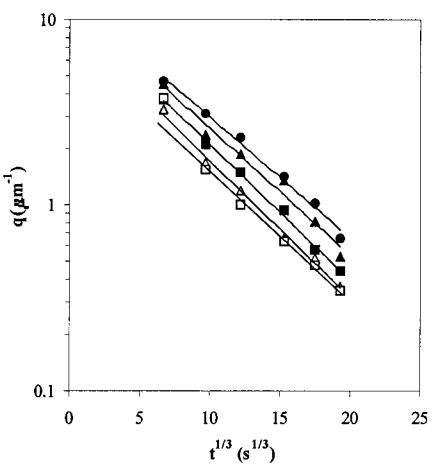

Figure 7 Plot of **q** versus $t^{1/3}$ at 170°C for all of the blends prepared at the critical compositions: (■) PE1/EcO2, (▲) PE2/EcO2, (●) PE3/EcO2, (□) PE1/EcO1, and (△) PE2/EcO1.

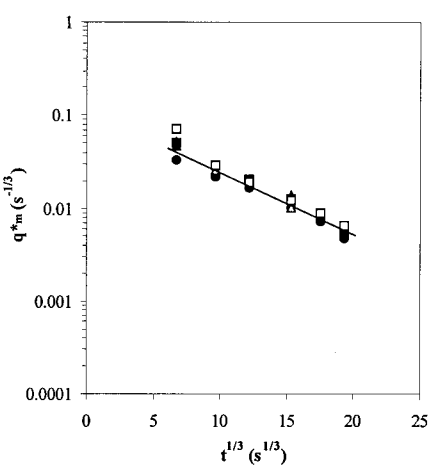

Figure 9 **q*** as a function of $t^{1/3}$ at 170°C: (■) PE1/EcO2, (▲) PE2/EcO2, (●) PE3/EcO2, (□) PE1/EcO1, and (△) PE2/EcO1.

function of the viscosity with little effect from the influence of molecular weight on the thermodynamic compatibilities of the blend constituents. In the study by Lee and Han[24] on the coarsening of the morphologies of immiscible polymer blends, it was explained, on the basis of Cahn's linearized theory of spinodal decomposition, that the length of morphology at very early times of coarsening was affected by the molecular weight of the constituent polymers. Higher molecular weights gave larger values of λ in the early stage compared with polymers with low molecular weight. In this work, the blends comprising polymers with the highest molecular weights showed the largest values of $\mathbf{q}$ and, hence, the smallest values of λ at the earliest times that were investigated. Moreover, the calculation of $\mathbf{q}^*$ largely removed the differences in $\mathbf{q}$ at the earliest times measured, indicating that at this stage, the coarsening process was controlled by the thermal energy and viscosity, thereby obscuring any effect of molecular weight on λ and $\mathbf{q}$.

Figure 10 shows an image of a PE1/EcO1 blend after 90 min of coarsening. Figure 11 shows the Fourier transform of the image with a ring pattern that indicates the presence of a regular pattern in the CCD image. The dimension of the pattern was of the order of 5 μm, that is, the λ of the blend morphology. Evidently, some remnants of the regular morphology produced during rapid precipitation from solution persisted at long t's in the melt state.

CONCLUSIONS

Blends prepared with compositions near the critical point through precipitation from solution formed regular cocontinuous morphologies that annealed at rates determined by the thermal energy and η_0^*. Data could be normalized with the function $\mathbf{q}^*$ such that the effects of thermal energy and viscosity largely accounted for differences in coarsening rate and, hence, showed that the differences in molecular weight had little effect on the compatibility of the blends and, therefore, the morphology.

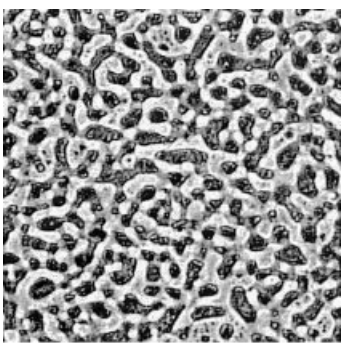

Figure 10 Regular coarsened morphology of a PE1/EcO1 blend prepared at the critical composition.

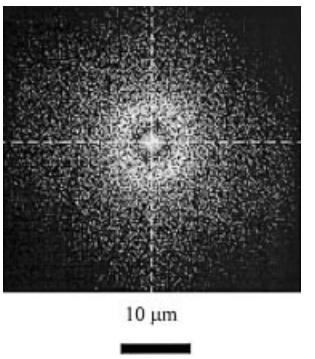

Figure 11 Fourier transform of the image in Figure 10, revealing the regular spacing of the domains in the morphology.

References

1. Mirabella, F. M. J Polym Sci Part B: Polym Phys 1994, 32, 1205.
2. Rhee, J.; Crist, B. J Polym Sci Part B: Polym Phys 1994, 32, 159.
3. Balsara, N. P.; Fetters, L. J.; Hadjichristidis, N.; Lohse, D. J.; Han, C. C.; Graessley, W. W.; Krishnamoorti, R. Macromolecules 1992, 25, 6137.
4. Weimann, P. A.; Jones, T. D.; Hillmayer, M. A.; Bates, F. S.; Londono, J. D.; Melnichenko, Y.; Wignall, G. D.; Almdal, K. Macromolecules 1997, 30, 3650.
5. Bates, F. S.; Schulz, M. F.; Rosedale, J. H. Macromolecules 1992, 25, 5547.
6. Rhee, J.; Crist, B. Macromolecules 1991, 24, 5663.
7. Inaba, N.; Yamada, T.; Suzuki, S.; Hashimoto, T. Macromolecules 1988, 21, 407.
8. Chen, C. Y.; Yunus, W. M. Z. W.; Chiu, H. W.; Kyu, T. Polymer 1997, 17, 4433.
9. Choi, P. Polymer 2000, 41, 8741.
10. Krishnamoorti, R.; Graessley, W. W.; Balsara, N. P.; Lohse, D. J. Macromolecules 1994, 27, 3073.
11. Saunders, K. J. Organic Chemistry of Polymers, 2nd ed.; Chapman & Hall: London, 1988; Chapter 2, p 46.
12. Chien, J. C. W.; He, D. J. J Polym Sci Part A: Polym Chem 1991, 29, 1585.
13. De Pooter, M.; Smith, P. B.; Dohrer, K. K.; Bennett, K. F.; Meadows, M. D.; Smith, C. G.; Schouwenaars, H. P.; Geerards, R. A. J Appl Polym Sci 1991, 42, 399.
14. Carreau, P. J. Ph.D. Thesis, University of Wisconsin, 1968.
15. Harris, D. C. J Chem Ed Chem Wisconsin Education 1998, 75, 119.
16. Dumoulin, M. M.; Utracki, L. A.; Carreau, P. J. In Two-Phase Polymer Systems; Utracki, L. A., Ed.; Hanser: Munich, Germany; Chapter 7, p 201.
17. Olley, R. H.; Basset, D. C. Polym Commun 1982, 23, 1707.
18. Hill, M. J.; Barham, P. J. Polymer 1995, 36, 3369.
19. Tabtiang, A.; Parchana, B.; Venables, R. A.; Inoue, T. J Polym Sci Part B: Polym Phys 2001, 39, 380.
20. Tabtiang, A.; Parchana, B.; Venables, R. A. Polym Plast Technol Eng 2001, 40, 423.
21. Crist, B.; Hill, M. J. J Polym Sci Part B: Polym Phys 1997, 35, 2329.
22. Cowie, J. M. G. Polymers: Chemistry and Physics of Modern Materials, 2nd ed.; Blackie Academic and Professional: London, 1991; Chapter 8, p 178.
23. Bicerano, J. Prediction of Polymer Properties; Marcel Dekker: New York, 1993; Chapter 3, p 66.
24. Lee, J. K.; Han, C. D. Polymer 1999, 40, 2521.
25. Cahn, J. W. J Chem Phys 1965, 42, 93.
26. Okamoto, M.; Shiomi, K.; Inoue, T. Polymer 1995, 36, 87.